Investigation of amorphous $Fe_{82}P_{11}B_7$ ultrafine particles produced by chemical reduction

1992 J. Phys.: Condens. Matter 4 6381

(http://iopscience.iop.org/0953-8984/4/30/005)

J. Phys.: Condens. Matter 4 (1992) 6381–6388. Printed in the UK

Investigation of amorphous $Fe_{82}P_{11}B_7$ ultrafine particles produced by chemical reduction

Jianyi Shen, Zheng Hu, Yuanfu Hsia† and Yi Chen

Department of Chemistry, Nanjing University, Nanjing 210008, People's Republic of China

Received 11 September 1991, in final form 6 April 1992

Abstract. $Fe_{82}P_{11}B_7$ ultrafine amorphous particles have been prepared by the reaction of Fe(III) chloride, sodium hypophosphite and potassium borohydride in aqueous solution. X-ray diffraction and electron diffraction indicated the amorphous nature of the sample and scanning electron microscopy showed that the sample consists of nearly spherical particles with diameters from 150 to 350 nm. X-ray photoelectron spectroscopy revealed that iron, phosphorus and boron existed mainly in their elemental states. The structure relaxation and crystallization of the amorphous sample were studied by Mössbauer spectroscopy after the sample had been annealed at various temperatures. The Mössbauer spectra suggested that the sample started to crystallize at 573 K; it crystallized completely through the formation of the α-Fe and $Fe_3(P_{0.6}B_{0.4})$ phases when the annealing temperature was raised to 673 or 773 K. When the annealing temperature is low (below 573 K), no crystalline phases can be detected but, as evidenced by the dependence of hyperfine field distribution $P(H)$ on annealing temperature, the heat treatment did cause a significant change in the microstructure of the amorphous sample.

1. Introduction

Studies on ultrafine amorphous alloy particles have attracted much attention because of their interesting intrinsic properties, e.g. short-range order, long-range disorder and high dispersion, as well as their important practical and/or potential applications, e.g. in powder metallurgy, magnetic materials, catalysts and ferrofluids. Increasing interest has been paid to the study of ultrafine amorphous alloy particles produced by chemical methods. Apart from the advantage of being applicable to large-scale production, chemical methods produce powder samples with characteristics quite different from ribbons and films obtained by liquid quenching or co-sputtering. The powder samples obtained by chemical reduction are highly dispersed and can be compacted to serve different purposes. The studies reported to date in the literature have been mainly limited to two systems, namely the Fe–C system formed by thermal decomposition of $Fe(CO)_5$ [1–4] and the Fe–M–B (M=Ni, Co, etc) system produced by the reduction of metal ions with borohydride in an aqueous solution [5–18]. It has already been established in the literature that the existence of the metalloid element strongly influences the nature of amorphous alloys [19]. To explore new systems containing metalloid elements other than carbon and boron seems valuable in order to attain a

† Present address: Department of Physics, Nanjing University, Nanjing 210008, People's Republic of China.

0953-8984/92/306381+08$04.50

better understanding of these complex systems. We report here an investigation of the fundamental properties of an a-$Fe_{82}P_{11}B_7$ sample produced by chemical reduction and its structure relaxation and crystallization after being annealed at various temperatures.

2. Experimental details

The Fe–P–B sample was prepared by mixing aqueous solutions of Fe(III) chloride, sodium hypophosphite and potassium borohydride at 273 K under ultrasonic agitation. In particular, the solutions of Fe(III) chloride (75 ml, 0.54 M) and sodium hypophosphite (75 ml, 1.07 M) were first mixed and the solution of potassium borohydride (150 ml, 1.36 M) was then added dropwise into the mixture. The black precipitate formed was washed thoroughly, first with deionized water and then with acetone to remove the soluble residue and water sequentially. The bulk composition of the sample obtained was analysed by an inductively coupled plasma method. The morphology and particle size of the sample were determined by scanning electron microscopy (SEM). X-ray diffraction (XRD) measurements were performed using Cu Kα radiation with a monochromator mounted on the diffracted beam. X-ray photoelectron spectroscopy (XPS) was used to analyse the electronic states of the elements on the surface. The sample was pre-treated by slightly bombarding it with 8 kV argon ions for 3 min before XPS measurement. The C 1s (284.6 eV) line was taken as a reference when calculating the binding energies. Differential scanning calorimetry (DSC) was performed in argon with a scanning rate of 20 K min^{-1} to investigate the crystallization process of the amorphous sample. The sample was also annealed in flowing high-purity nitrogen for 2 h at given temperatures from 373 to 773 K at intervals of 100 K. Mössbauer spectra were then recorded on a constant-acceleration spectrometer with a source of 15 mCi ^{57}Co in a Pd matrix. The magnetic hyperfine field distribution of the amorphous species was obtained according to their broadened Mössbauer spectra by using the method described by Le Caër and Dubois [20] and the $S^1(\Delta)$-type peak shape was adopted in the data fitting. The Mössbauer spectra of the crystallized species were fitted with the MOSFUN program developed by Muller [21] and the peak area ratio of the sextuplets was constrained to 3:2:1:1:2:3. The Mössbauer data were calculated with respect to α-Fe.

3. Results and discussion

Figure 1 shows the XRD pattern of the as-prepared sample. Only a broad 2θ peak near 45° can be seen, indicating the amorphous structure of the sample. This result is further evidenced by the broad and diffuse Debye rings of the selected-area electron diffraction image of the sample as shown in figure 2. The Mössbauer spectrum of the as-prepared sample, as shown later in figure 6, curve a, consists of six broadened lines with a distribution of magnetic hyperfine fields in the sample due to its long-range disorder. The magnetic hyperfine field distribution of the as-prepared sample, as expressed by $P(H)$ versus H, is shown later in figure 7, curve a, and the mean hyperfine field value was found to be 235 kOe, which indicated that iron was in its metallic state in the as-prepared sample.

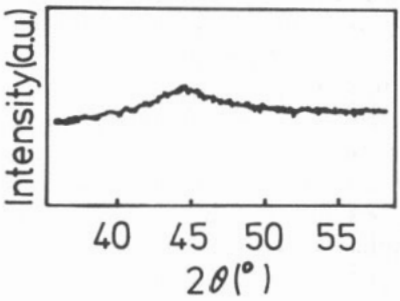

Figure 1. XRD pattern of $Fe_{82}P_{11}B_7$ ultrafine alloy particles (a.u., arbitrary units).

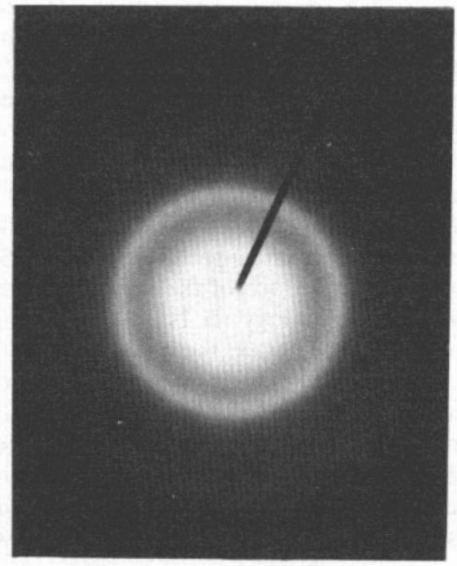

Figure 2. Selected-area electron diffraction image of $Fe_{82}P_{11}B_7$ ultrafine alloy particles.

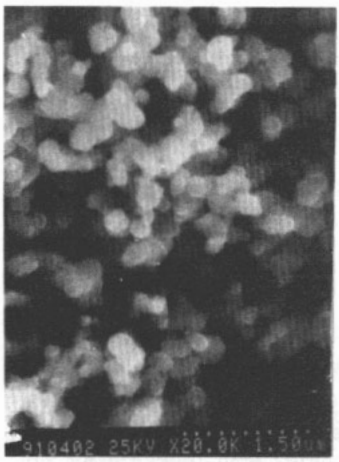

Figure 3. SEM of $Fe_{82}P_{11}B_7$ ultrafine amorphous particles.

As can be seen in the SEM photograph in figure 3, the sample consists of nearly spherical particles with diameters ranging from 150 to 350 nm, which is in the 'ultrafine' range (less than 1 μm).

XPS results for the as-prepared sample are shown in figure 4. In figure 4, curve a, two main peaks of iron with binding energies of 706.7 eV and 719.9 eV are attributed to the Fe $2p_{3/2}$ and Fe $2p_{1/2}$ levels, respectively. The binding energy of 706.7 eV for Fe $2p_{3/2}$ is consistent with the values for Fe–B and pure iron metal [22]. In addition, a shoulder peak with a binding energy of around 710 eV can be assigned to the oxidized iron species on the surface. The relative areas of the main and shoulder

peaks of the Fe $2p_{3/2}$ level suggest that iron exists mainly in its metallic state on the surface of the sample. Figure 4, curve b, is the XPS spectrum of the P 2p level on the surface of the sample. The peak with a lower binding energy of 129.4 eV arises from the elemental phosphorus bounded to metallic iron, while the peak with the higher energy of 133.5 eV can be assigned to the oxidized phosphorus species, which are in accordance with the values of the P 2p level in the a-NiP system [22]. The binding energy of 129.4 eV for the P 2p level in our sample is smaller than that of red phosphorus (130.0 eV). The chemical shift of −0.6 eV results from the electron transfer from iron to phosphorus [22]. Similarly, two boron species have also been found on the surface of the sample. As shown in figure 4, curve c, the peak with the lower binding energy (B 1s; 187.2 eV) can be related to the elemental boron bound to metallic iron, while the peak with the higher binding energy (B 1s; 191.4 eV) can be attributed to the oxidized boron species on the surface of the sample [12, 22]. Okamoto *et al* [22] found positive shifts for the binding energies of the elemental boron species in a-NiB and a-FeB samples, and the deviations were due to electron donation from boron to the metals. However, no positive chemical shift has been found for the elemental boron species in our sample. This result may reflect the existence of complicated interactions between iron, phosphorus and boron.

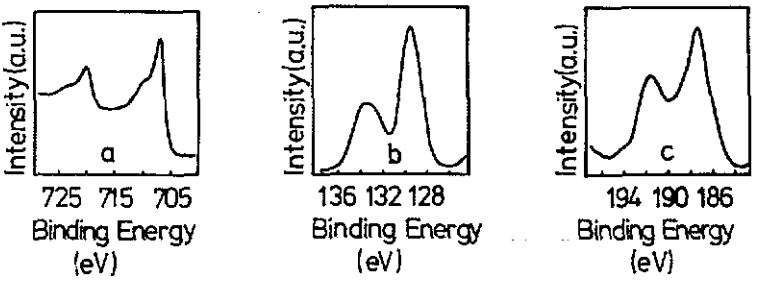

Figure 4. X-ray photoelectron spectra of the Fe $2p_{1/2}$ and Fe $2p_{3/2}$ levels (curve a), the P 2p level (curve b) and the B 1s level (curve c) in $Fe_{82}P_{11}B_7$ ultrafine amorphous particles (a.u., arbitrary units).

The common feature of the XPS results of the three components is that they all have been partially oxidized on the surface during preparation. However, the relative amounts of the oxidized species are low as estimated by the relative peak areas of the oxidized and corresponding elemental species in their XPS spectra. Since it is well known that the surface atoms are more easily oxidized than those in the bulk, it seems reasonable to consider that the component elements iron, phosphorus and boron in the bulk phase of the sample are all in their elemental states.

DSC was carried out to help to characterize the crystallization process of the $Fe_{82}P_{11}B_7$ sample and an ultrafine amorphous alloy sample of $Fe_{87}B_{13}$ was used for comparison. As shown in figure 5, both samples give only one exothermal peak but with different peak temperatures. The $Fe_{82}P_{11}B_7$ sample has a peak temperature at 718 K, which is lower than that of the $Fe_{87}B_{13}$ sample (757 K). The results suggest that, in comparison with boron, phosphorus may reduce the crystallization temperature of the sample. The heats of crystallization of $Fe_{87}B_{13}$ and $Fe_{82}P_{11}B_7$ are 67.8 J g^{-1} and 83.4 J g^{-1}, respectively, which are of the same order.

The structure relaxation and crystallization of the $Fe_{82}P_{11}B_7$ sample have been studied by Mössbauer spectroscopy. The room-temperature Mössbauer spectra for

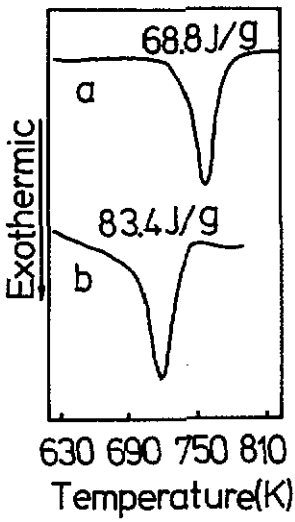

Figure 5. DSC curves of $Fe_{87}B_{13}$ (curve a) and $Fe_{82}P_{11}B_7$ (curve b) ultrafine amorphous particles.

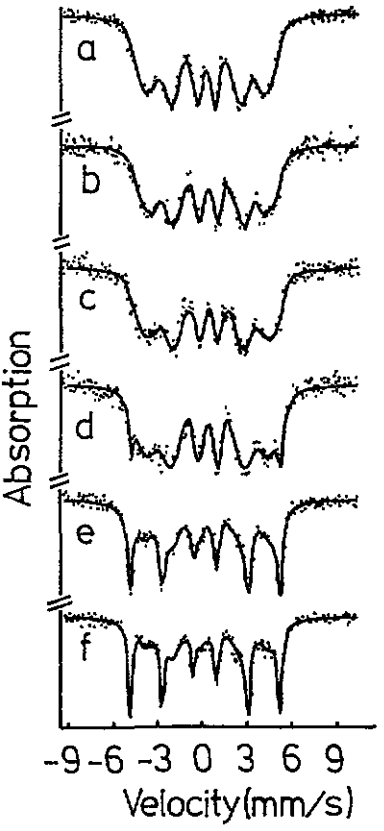

Figure 6. Room-temperature Mössbauer spectra of $Fe_{82}P_{11}B_7$ ultrafine amorphous particles as prepared (curve a) and annealed in N_2 for 2 h at 373 K (curve b), 473 K (curve c), 573 K (curve d), 673 K (curve e) and 773 K (curve f).

Table 1. Mössbauer parameters of the amorphous $Fe_{82}P_{11}B_7$ sample treated in N_2 for 2 h at 373, 473 and 573 K. $R = I(m_e = \pm\frac{1}{2})/I(m_e = \pm\frac{3}{2})$ is the intensity ratio of the $m_e = \pm\frac{1}{2}$ line to the $m_e = \pm\frac{3}{2}$ line.

Temperature (K)	$\langle H \rangle$ (kOe)	R	Amorphous phase (%)
(As prepared)	235	0.55	100
373	240	0.61	100
473	243	0.41	100
573	257	0.66	94

the as-prepared sample and for the sample which had been annealed in high-purity N_2 at various temperatures are shown in figure 6, and the Mössbauer parameters with respect to α-Fe are listed in tables 1 and 2. As shown in figure 6, curve d, the sample partially crystallized after annealing at 573 K with the appearance of a crystalline phase of α-Fe, which has a spectral contribution of about 6%. The Mössbauer spectra

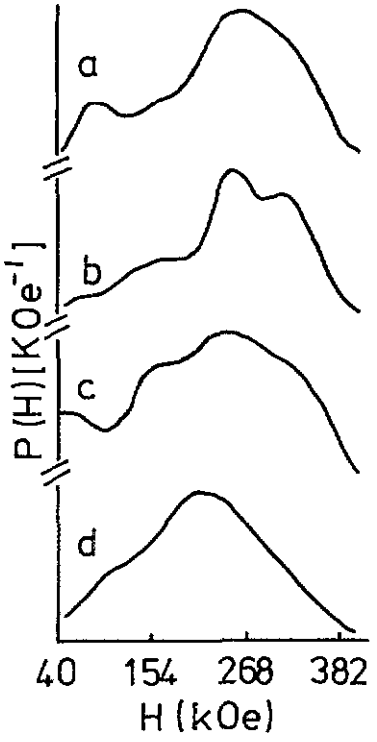

Figure 7. Hyperfine field distributions in $Fe_{82}P_{11}B_7$ ultrafine amorphous particles as prepared (curve a) and annealed in N_2 for 2 h at 373 K (curve b), 473 K (curve c) and 573 K (curve d).

Table 2. Mössbauer parameters of the amorphous $Fe_{82}P_{11}B_7$ sample treated in N_2 for 2 h at 673 and 773 K.

Temperature (K)	H (kOe)	IS (mm s^{-1})	Assignment	Site	Area (%)
673	331	0.01	α-Fe		32
	288	0.21		I	
	244	0.26	$Fe_3(P_{0.6}B_{0.4})$	II	68
	187	0.37		III	
773	331	0.01	α-Fe		36
	285	0.24		I	
	245	0.26	$Fe_3(P_{0.6}B_{0.4})$	II	64
	184	0.42		III	

of the sample after annealing at 373 and 473 K are similar to that of the as-prepared sample as shown in figure 6, curves a–c, indicating that, at temperatures lower than 573 K, annealing does not cause crystallization of the sample. However, as shown in figure 7, the hyperfine field distribution $P(H)$ of the sample annealed at various temperatures changes dramatically, demonstrating that relaxation of the amorphous structure does occur. The $P(H)$-curve of the as-prepared sample is mainly composed of two peaks, reflecting the existence of different domains with different short-range orders in the sample. The peak at a low field may arise from domains that have high concentrations of metalloid elements, while the other distribution peak at a high

field is asymmetric and similar to that of $Fe_{80}P_{20}$ ribbon [19]. Interestingly, with the increase in the annealing temperature from 373 to 573 K, the main high-field $P(H)$ peak first splits at 373 K and gradually shifts towards a lower field while the low-field peak gradually disappears and, as a result, the mean hyperfine field increases (cf table 1). This can be explained by the diffusion of the elements in the sample during the heat treatment. It seems reasonable to assume that, by heat treatment, the metalloid elements diffuse from domains with a high concentration to domains with a low concentration, while part of the iron gradually separates to form crystalline α-Fe. The remaining amorphous phase tends to become homogeneous in chemical composition with an Fe-to-P+B ratio of 3; this is expected to be stable because both crystalline Fe_3B and Fe_3P are stable.

Table 3. Comparison between Mössbauer parameters for Fe_3P, Fe_3B and $Fe_3(P_{0.6}B_{0.4})$.

Phase	Site	IS (mm s^{-1})	H (kOe)	Data source
Fe_3P	I	0.30	279	
Fe_3P	II	0.30	240	[23][a]
Fe_3P	III	0.35	174	
Fe_3B	I	0.14	286	
Fe_3B	II	0.08	267	[14]
Fe_3B	III	0.16	223	
$Fe_3(P_{0.6}B_{0.4})$	I	0.24	282	
$Fe_3(P_{0.6}B_{0.4})$	II	0.21	251	Calculated [b]
$Fe_3(P_{0.6}B_{0.4})$	III	0.27	194	
$Fe_3(P_{0.6}B_{0.4})$	I	0.21	288	Measured in this
$Fe_3(P_{0.6}B_{0.4})$	II	0.26	244	study (figure 6, curve e)
$Fe_3(P_{0.6}B_{0.4})$	III	0.37	187	

[a] Average values are used here.
[b] Calculated from the values for Fe_3P and Fe_3B above, weighted by the content of P and B in $Fe_3(P_{0.6}B_{0.4})$.

The Mössbauer spectrum of the sample annealed at 673 K is shown in figure 6, curve e, which clearly indicates complete crystallization of the sample. The spectrum can be fitted with four sextets. Their corresponding parameters are listed in table 2. Besides the typical sextet for α-Fe, the other three sextets with hyperfine fields of 288, 244 and 187 kOe may result from iron atoms in three inequivalent lattice positions of crystalline Fe–P–B species. If we take into consideration the relative absorption intensities of α-Fe (32%) and the crystalline Fe–P–B species (68%), together with the P and B contents in the sample, it is found that the species can be expressed by $Fe_3(P_{0.6}B_{0.4})$, which can be taken as a mixture of the isostructural Fe_3P and Fe_3B or as an isostructural species with P and B atoms randomly distributed in the three inequivalent lattice positions. As can be seen in table 3, most values for the isomer shift and hyperfine field of the three sextets are located between the corresponding values of Fe_3B and Fe_3P [14, 23]. Included in table 3 are also the calculated parameters for the three sextets of $Fe_3(P_{0.6}B_{0.4})$ based on the reference parameters of Fe_3P and Fe_3B weighted in the ratio of 0.6:0.4, and the parameters obtained by fitting the Mössbauer spectrum of the sample which had been annealed

at 673 K. It is clearly shown that the experimental values are basically consistent with the calculated values with experimental errors of ± 0.02 mm s^{-1} for the isomer shift and ± 5 kOe for the hyperfine field. If the spectrum is fitted with six sextets, it may be possible to distinguish the iron atoms for Fe_3P and Fe_3B, respectively, in the sample.

Increasing the annealing temperature to 773 K brought about basically the same results as for the sample annealed at 673 K (cf figure 6, curve f, and table 2).

References

[1] van Wonterghem J, Mørup S, Charles S W, Wells S and Villadsen J 1985 *Phys. Rev. Lett.* **55** 410
[2] van Wonterghem J, Mørup S, Charles S W, Wells S and Villadsen J 1986 *Hyperfine Interact.* **27** 333
[3] Mørup S, Christensen B R, van Wonterghem J, Madsen M B, Charles S W and Wells S 1987 *J. Magn. Magn. Mater.* **67** 249
[4] van Wonterghem J, Mørup S, Charles S W, Wells S 1988 *J. Colloid Interface Sci.* **121** 558
[5] van Wonterghem J, Mørup S, Koch C J W, Charles S W and Wells S 1986 *Nature* **322** 622
[6] Linderoth S, Mørup S, Meagher A, Larsen J, Bentzon M D, Clausen B S, Koch C J W, Wells S and Charles S W 1989 *J. Magn. Magn. Mater.* **81** 138
[7] Linderoth S, Mørup S and Bentzon M D 1990 *J. Magn. Magn. Mater.* **83** 457
[8] Linderoth S, Mørup S, Koch C J W, Wells S, Charles S W, van Wonterghem J and Meagher A 1988 *J. Physique Coll.* **49** C8 1369
[9] Mørup S, van Wonterghem J, Meagher A and Koch C J W 1987 *IEEE Trans. Magn. Magn.* **23** 2978
[10] van Wonterghem J and Mørup S 1988 *Hyperfine Interact.* **42** 959
[11] Inoue A, Saida J, Masumoto T 1988 *Metall. Trans.* A **19** 2315
[12] Corrias A, Ennas G, Licheri G, Marongiu G, Musinu A, Paschina G, Piccaluga G, Pinna G and Magin M 1988 *J. Mater. Sci. Lett.* **7** 407
[13] Wells S, Charles S W, Mørup S, Linderoth S, van Wonterghem J, Larsen J and Madsen M B 1989 *J. Phys.: Condens. Matter* **1** 8199
[14] Jiang J, Zhao F, Gao P, Dezsi I and Gonser U 1990 *Hyperfine Interact.* **55** 981
[15] Jiang J, Dezsi I, Gonser U and Lin X 1990 *J. Non-Cryst. Solids* **124** 139
[16] Li F S, Xue D S and Zhou R J 1990 *Hyperfine Interact.* **55** 1021
[17] Dragieva I, Rusev Kr and Stanimirova M 1990 *J. Less-Common Met.* **158** 295
[18] Hu Z, Hsia Y, Zheng J, Shen J, Yan Q and Dai L 1991 *J. Appl. Phys.* **70** 436
[19] Musser D, Chien C L and Chen H S 1979 *J. Appl. Phys.* **50** 7659
[20] Le Caër G and Dubois J M 1979 *J. Phys. E: Sci. Instrum.* **12** 1083
[21] Muller E W 1981 *Mössbauer Effect Reference Data J.* **4** 89
[22] Okamoto Y, Nitta Y, Imanaka T and Teranishi S 1979 *J. Chem. Soc. Faraday Trans.* I **75** 2027
[23] Lisher E J, Wilkinson C, Ericsson T, Haggstrom L, Lundgren L and Wappling R 1974 *J. Phys. C: Solid State Phys.* **7** 1344